

This discussion paper is/has been under review for the journal Atmospheric Chemistry and Physics (ACP). Please refer to the corresponding final paper in ACP if available.

Seasonal variation of black carbon over the South China Sea and in various continental locations in South China

D. Wu¹, C. Wu², B. Liao¹, F. Li¹, H. Tan¹, T. Deng¹, H. Li¹, H. Chen¹, D. Jiang¹, and J. Z. Yu^{2,3,4}

¹Institute of Tropical and Marine Meteorology, CMA, Guangzhou 510080, China

²Division of Environment, Hong Kong University of Science and Technology, Clear Water Bay, Kowloon, Hong Kong, China

³Atmospheric Research Centre, Fok Ying Tung Graduate School, Hong Kong University of Science and Technology, Nansha, Guangzhou, China

⁴Department of Chemistry, Hong Kong University of Science and Technology, Clear Water Bay, Hong Kong, China

Received: 13 May 2013 – Accepted: 16 June 2013 – Published: 1 July 2013

Correspondence to: D. Wu (wudui@grmc.gov.cn) and J. Z. Yu (chjianyu@ust.hk)

Published by Copernicus Publications on behalf of the European Geosciences Union.

17375

Abstract

Black carbon (BC) is an important atmospheric constituent as an air pollutant and as a climate forcer. To our knowledge, field measurements of BC have not been reported over the South China Sea. Observation of light absorption coefficients (σ_{abs}) and BC concentrations by Aethalometer were conducted on Yongxing Island in the South China Sea and at five continental sites in the Pearl River Delta (PRD) region, South China during the South China Sea monsoon period (rainy season, 16 May–20 June 2008) and the northeast monsoon period (dry season, 12 December 2008–8 January 2009). At the oceanic site, the daily average BC concentrations vary from 0.28 to 2.14 $\mu\text{g m}^{-3}$ and seasonal variations of BC were small (0.67 in dry season and 0.54 $\mu\text{g m}^{-3}$ in rainy season). Similarly, little seasonal difference was found at a background site in PRD (2.88 in dry season and 2.62 $\mu\text{g m}^{-3}$ in rainy season). At PRD urban sites, the daily average concentration of BC ranges from 1.56 to 37.9 $\mu\text{g m}^{-3}$, higher in the dry season (12.6 $\mu\text{g m}^{-3}$) and lower in the rainy season (6.4 $\mu\text{g m}^{-3}$). The observed average σ_{abs} values in rainy vs. dry seasons are 119 vs. 62 Mm^{-1} at the PRD urban sites, 29 vs. 26 Mm^{-1} at the PRD background site, and 8.4 vs. 7.2 Mm^{-1} at the marine site. A bi-peak pattern in diurnal BC variation was observed at all sites while this pattern is the most prominent at the urban sites. The first peak appears in the early morning rush hour and the second peak in early evening, with the evening peak more pronounced in dry season.

1 Introduction

Aerosol, as an important climate forcer, has attracted increasing attention in the atmospheric research community (Lohmann and Lesins, 2002; Menon et al., 2002; Penner et al., 2004). Atmospheric aerosols scatter and absorb solar radiation, thus significantly impacting the climate (Babu and Moorthy, 2001; Reddy and Venkataraman, 2000). Black carbon (BC) is an important component of atmospheric aerosols, affecting visi-

17376

bility, cloud formation, cloud cover and lifetime. IPCC started reporting radiative forcing due to BC aerosol since its second report (IPCC, 1996). The heating effect of BC aerosols may offset the cooling effect of sulfate and mineral aerosols (Andreae, 2001). If the mixing state of BC is taken into account, the radiative forcing of BC is estimated to be sufficiently strong to make BC the third global warming contributor after CO₂ and CH₄ (Jacobson, 2001). BC aerosols could also have a significant impact on regional climate change (Ramanathan and Carmichael, 2008).

In China, a number of recent projects have focused on carbon aerosol, including projects sponsored by the National Natural Science Foundation of China and various international cooperation research projects. Chinese researchers have studied various aspects of BC aerosols, such as the physical characteristics, optical properties, sources, temporal and spatial distribution and the impact on the environment and climate, using multiple approaches including field observations, laboratory investigations, numerical simulation and theoretical investigations. Since 1990s, a large body of observational data of BC aerosols in China has accumulated through field measurements. Tang et al. (1999) reported short-term observations of BC concentrations in Lin'an (a background station) in 1991 and in the Lasha area in 1998. Wang et al. (2005) measured BC concentrations in the northern suburbs of Beijing in 1992 and for the period of 1996–2004. In 1994, China's first global background atmospheric observatory was established in the Waliguan Mountains of Qinghai at 3810 m.a.s.l., and the research carried out there has produced valuable findings related to BC (Qin et al., 2001). Chi et al. (2000) reported seasonal variation in abundance of elemental carbon (EC) in Beijing measured using a CHN analyzer. They found that higher EC in winter may be related to heating. Research in Qiqihar City found a similar seasonal variation pattern (Sun et al., 1997). Zhu et al. (1996) studied EC particle size distributions in Pudong, Shanghai. Cao et al. (2004) reported high organic carbon (OC) and EC concentrations in PM₁₀ and PM_{2.5} across the Pearl River Delta (PRD) region, measured using the IMPROVE protocol on a DRI carbon analyzer. Their results suggested significant impact of emissions from motor vehicles on ambient EC loadings (Cao et al., 2004).

17377

Lou et al. (2005) measured BC in PM_{2.5}, PM₁₀ and TSP in Beijing using a filter-based light absorption technique and found that most BC was in PM_{2.5}. In late 2003, our group launched light absorption measurement using Aethalometers (Magee Scientific Company, Berkeley, CA, USA) and filter-based EC measurement by thermal/Optical analysis in the PRD region.

Asian BC aerosol also attracted attention of scientists worldwide due to its widespread and increasing atmospheric abundance. In 1999, European and American scientists found that southern Asia is often shrouded in a brown cloud of aerosols 3 km thick, referred to as the Asian Brown Cloud by many researchers (Ramanathan et al., 2002; Engling and Gelencser, 2010). In China, this phenomenon is often simply referred to as "haze" (Wu, 2005; Wu et al., 2005, 2007). Later, the similar phenomenon was found over every continent, more commonly known as the atmospheric brown cloud. The widespread presence of BC suggests that the role of BC as a warming forcing needs to be studied in order for the assessment of aerosol's role in global and regional climate change (Ramanathan and Carmichael, 2008) and for the attribution of contributions by individual countries. It has become clear that high-resolution spatial and temporal observations of radiation parameters of aerosol are essential data for assessment of the impact of Chinese aerosols on global and regional climate change.

In this work, we report BC and aerosol light absorption measurements by Aethalometers and their seasonal variations in 2008 in a remote location over the South China Sea and six continental locations in South China. The marine location is Yongxing Island (YX) of the Xisha Islands in the South China Sea. The continental locations include Nancun (NC), Panyu (PY), Xinken (XK) and Mt. Maofeng (Maofengshan (MFS) in Chinese), Dongguan (DG) in the PRD region in Guangdong Province and Yangshuo (YS) in Guangxi Zhuang Autonomous Region. PRD, the second largest delta in China, has been one of the fastest growing economic areas for nearly 30 yr and among the most polluted areas in China. PRD has a total land area of 8000 km² and a high population density. It is home to multiple mega cities including Guangzhou, Hong Kong, Shenzhen, Dongguan, Macao, Zhuhai, and Foshan. The urbanization in PRD has led

17378

to vegetation reduction, increased demand in transportation, and blooming of township enterprises, which in turn have resulted in increasingly frequent air pollution episodes (Wu et al., 2005).

5 Southern Mainland China is in a subtropical monsoon climate and the northern part of the South China Sea (SCS) is in a tropical monsoon climate. Controlled by the northeast monsoon, October to April in the following year is the dry season of southern China. Affected by the South China Sea monsoon, May to September is the rainy season.

2 Field observations

10 2.1 Sampling locations

The Institute of Tropical and Marine Meteorology (ITMM) started to establish a monitoring network for atmospheric compositions over the PRD region in 2003, and since that time a total of nine monitoring stations have been established. The observations presented in this paper include data from five long-term stations (NC, PY, XK, MFS, 15 and DG) in PRD and two short-term stations outside PRD in South China. The station locations are shown in Fig. 1. Among the stations, NC, PY, XK and MFS are located in different districts in the city Guangzhou, the biggest mega-city in southern China. The MFS station is located on the top of Mt. Maofeng (535 m a.s.l.) and 20 km northeast to downtown Guangzhou. MFS, due to its high altitude and its rural location, represents the background condition of the PRD region. NC is a suburban site in the center of the PRD and the NC station is situated on the top of the highest peak (141 m a.s.l.) in Guangzhou's Panyu district. At 141 m a.s.l., this station is less impacted by ground-level local emissions, thus approximately representing the average atmospheric mixing characteristics in the PRD region. PY is an urban surface site and 7 km southwest 20 to NC station, representing urban conditions in Guangzhou. Due to a busy road only 140 m away from the station, significant influence of vehicular emissions is expected for

17379

the PY site. XK is a rural surface site, 60 km south to downtown Guangzhou. The prevailing northerly winds in winter make XK a receptor site of pollution in Guangzhou. DG is in a suburban neighborhood in the city Dongguan, one of the largest manufacturing centers in China.

5 The two short-term observation stations are YS in Guangxi and YX Island in the middle of the South China Sea. YS is a small tourist city, surrounded by mining and metallurgical industries in the area. YX island has an elevation of 5.6 m, an area of 1.82 km² and a population of ~ 500. The distance between YX Island and the center of PRD is approximately 730 km. YX represents the average situation of the tropical area 10 over the Southern China Sea. It is noted that YX island is en route of marine vessels travelling from middle-east, Africa and Europe to East Asia (Kaluza et al., 2010).

Observations reported in this work were carried out in two periods, 16 May–20 June 2008 in the rainy season and 12 December 2008–8 January 2009 in the dry season. Due to a lack of measurement instruments, the same instrument was first 15 deployed to YS from 16 May to 21 May then moved to YX for the remaining rainy season observation. The instrument remained at YX for the dry season observation, thus no observation was made at YS in the dry season.

2.2 Sampling instruments

In this study, six Aethalometers (AE-31-HS, AE-31-ER, and AE-16-ER, Magee Scientific Company, Berkeley, CA, USA) were deployed to determine aerosol absorption coefficients and BC concentrations. The AE-31 models measure light attenuation at seven 20 wavelengths, i.e., 370, 470, 520, 590, 660, 880, and 950 nm. The AE-16 model has only one measurement channel at 880 nm. These instruments were operated to provide continuous observations with a time resolution of 5 min. Light attenuation measured by 25 Aethalometers is dominated by BC, as other constituents in the atmospheric particles absorb negligible amount of solar radiation at visible and infrared range (Moosmuller et al., 2009). BC concentration is then derived from the attenuation measurement by adopting specific values for attenuation cross-section. The latter was obtained from

17380

comparison of attenuation and EC mass, which was determined to be 16.6 using a thermal analysis method developed in Lawrence Berkeley Laboratory (LBL) (also known as evolved gas analysis method) (Gundel et al., 1984) and used in the Aethalometers in reporting BC. It should be noted that Aethalometer BC is not equivalent to EC determined using the more widely adopted NIOSH or IMPROVE thermal/optical protocol.

The Aethalometers were installed inside containers, with their inlets located 2 m above the container roof. A conductive silicone tubing (TSI, Shoreview, MN, USA) was used in the inlet system to minimize particle losses due to static charge. The Aethalometer deployed in YS and YX Island during the rainy season were equipped with a 2.5 μm cyclone while a 10 μm cyclone was used for the instruments at the other stations. The sampling flow rate was either 3 or 5 L min^{-1} (Wu et al., 2009). Routine flow calibration and blank tests were performed before sampling. A threshold value of attenuation for the periodical advancing of the filter tape was set at 100.

Measurements of σ_{abs} and BC by the Aethalometers deployed in this study are applied for a correction factor derived from an inter-instrument comparison exercise. In 2004, we made two sets of side-by-side observations, one set using an Aethalometer (880 nm) and a Photo-acoustic Spectrometer (PAS, 532 nm) from Max Planck Institute in a downtown location in Guangzhou, and the second set using an Aethalometer and a Multi-Angle Absorption Photometry (Carusso/MAAP, 637 nm) in a rural location near Guangzhou at the same time. The photo-acoustic method is more accurate in determining light absorption than the filter-based method, which may be subject to sampling artifacts linked to aerosol loading, filter matrix, and scattering effect (Coen et al., 2010). The light absorption measurement between Aethalometer and PAS is well correlated and an empirical formula as shown below is obtained (Wu et al., 2009):

$$\sigma_{\text{PAS}, 532 \text{ nm}} = 0.51\sigma_{\text{AE}, 880 \text{ nm}} + 0.82 \quad (1)$$

Where $\sigma_{\text{PAS}, 532 \text{ nm}}$ is the light absorption coefficient at 532 nm measured by PAS and $\sigma_{\text{AE}, 880 \text{ nm}}$ is the light absorption coefficient at 880 nm measured by the Aethalometer. Similarly, an empirical formula was obtained to relate BC mass measurements by

17381

MAAP and the Aethalometer (Wu et al., 2009):

$$\text{BC}_{\text{MAAP}} = 0.897 \times \text{BC}_{\text{AE}} - 0.062 \quad (2)$$

σ_{abs} reported in this work have been corrected with Eq. (1) while BC mass have been corrected using Eq. (2).

Aethalometers report both σ_{abs} and BC. It is important to keep in mind that σ_{abs} is what Aethalometers directly measure while BC concentrations by Aethalometer are derived from σ_{abs} measurement assuming that Mass Absorption Efficiency (MAE) of BC aerosol is a constant during the sampling period. However, in reality MAE varies in time and space, depending on the mixing state of BC. As a result, BC concentration data have additional uncertainties due to the uncertainty introduced by the constant multiplier (MAE). As there is a larger community interested in BC mass concentrations, data in this paper are mainly presented in the form of BC mass concentrations. The detailed results of light absorption measurements are provided as Supplement.

3 Results

3.1 BC time series

Hourly variations of BC and meteorological parameters during the measurement campaigns are shown in Fig. 2a for the rainy season and Fig. 2b for the dry season. Concentration distributions in the form of histograms are also shown next to the respective time series plots in Fig. 2. The histograms show that YX has the sharpest frequency distribution among all sites in both the rainy and dry seasons as a result of small temporal variation in BC concentrations. The weak temporal variation characteristic confirmed the nature of YX as a super-regional background site. For most of time, BC in YX was at a low level of $\sim 0.5 \mu\text{g m}^{-3}$ in the rainy season and $\sim 0.6 \mu\text{g m}^{-3}$ in the dry season. A few concentration spikes were observed in YX during the sampling campaign. The

17382

cause of these episodic events was investigated by examining σ_{abs} at different wavelength. Absorption Angstrom Exponent (AAE) can be considered as an indicator of mixing state. AAE of pure BC is close to 1 (Moosmuller et al., 2011) and the value increases as BC mixes with either light absorbing organic carbon (i. e., brown carbon (BrC)) (Kirchstetter et al., 2004) or non-light absorbing materials such as sulfate (Lack and Cappa, 2010). Usually the AAE of BC, when mixing with BrC, could increase to > 1.6, which is more significant than when mixing with non-light absorbing materials (AAE < 1.6). The observed average AAE in YX was 0.97 in rainy season and 1.06 in dry season (Fig. S4). The AAE values are close to unity, suggesting the negligible influence from biomass burning, which otherwise would lead to significantly elevated AAE due to atmospheric processing of BC particles. This level of AAE is lower than those found over the East China Sea (1.3) (Chung et al., 2012). The temporal variations of AAE and σ_{abs} (Fig. S5) show that the AAE varied from 0.5 to 2 during the sampling period, but the AAE variation was much smaller during two episodic events (14–17 December 2008 and 1–3 January 2009, highlighted in yellow in Fig. S5). This phenomenon suggests that the elevated σ_{abs} during the episodes were likely influenced by more “fresh soot” (such as a passing ship) in comparison to those on the regular days.

MFS is downwind of the PRD urban areas in the rainy season and upwind of the PRD urban areas in the dry season. The measurements indicated that BC variations in MFS were independent of the other PRD sites in rainy season, as shown in Fig. 2 and also evidenced by the low inter-site correlations in Table 1. This result suggests that transport of BC from ground level to an altitude as high as that of MFS (435 m) was not effective. In the dry season, BC in MFS was weakly correlated with the urban sites PY and NC. The weak BC influence from the source region of PRD on MFS supports the characterization of MFS as a site representing the PRD background conditions. The BC data histogram at MFS in rainy season is different from those at the other sites, most likely related to the intermittent data at MFS (Fig. 2a).

NC, located at an altitude of 141 m, could represent the average mixing conditions of air pollutants in the urban region of Guangzhou. This is supported by the high correla-

17383

tions of BC at NC with BC at PY, XK and even DG (Table 1). In the rainy season, the BC variation trend at NC is very similar to those at PY and DG, and the latter two areas are among the major BC source regions in PRD. The total precipitation was ~ 450 mm in the rainy sampling period, accounting for ~ 30 % of the annual precipitation. The BC reduction was not significant after rain events (Fig. 2a), implying that wet deposition was not the major cause for lower BC in the rainy season. In the dry season, BC variation trend at NC was similar to that at DG and a higher inter-site correlation was observed between the two sites (r : 0.72 in the dry season vs. 0.66 in the rainy season).

In the rainy season, stronger dispersion condition (wind speed: 2.91 ms^{-1} in the rainy season vs. 2.15 ms^{-1} in the dry season) along with abundant rainfall, resulted in stronger removal of BC from the atmosphere in the source region. By comparison, the less removal of BC in dry season makes the diurnal variations of BC at PY more closely track the diurnal pattern of transportation emissions. As a result, a broader concentration distribution histogram was observed at PY in dry season than at other sites, consistent with the site characteristic of PY being in close proximity to sources. At XK, a much smaller percentage of valid data was obtained in the rainy season due to instrument problems. Consequently, only measurements in the dry season are discussed for XK. In the dry season, the prevailing northeasterly wind in the PRD region places XK downwind of both DG and NC. BC in XK was well correlated with DG and NC during dry season, consistent with the source–receptor relationship among the sites. It is also noted that higher BC level was observed at the rural site XK than that at the suburban surface site DG. This may suggest that there were additional strong BC sources impacting XK.

3.2 Spatial variation in BC

The spatial variation in seasonal average BC concentrations is shown in Fig. 1, with the highest BC occurring at the surface sites in PRD, followed by the sites at elevated altitudes (i.e., NC and MFC), and the lowest BC at the oceanic site YX Island. The limited measurements of BC in YS, Guangxi in the rainy season indicated the average

17384

BC ($6.93 \mu\text{g m}^{-3}$) at this site is comparable to those observed at the PRD urban locations. The unexpectedly high level of BC in YS, considering it is mainly a tourist town, may suggest that emissions from nearby mining and metallurgical industries had a significant impact on BC level at YS. The daily average concentration of BC varied from 0.21 to $2.14 \mu\text{g m}^{-3}$ at the oceanic site YX Island, 0.71 to $5.43 \mu\text{g m}^{-3}$ at the PRD regional background site MFS, 2.33 to $15.97 \mu\text{g m}^{-3}$ at the elevated site NC, and 1.56 to $37.9 \mu\text{g m}^{-3}$ among the ground sites in South China. In the dry season, the average BC reached as high as $12.65 \mu\text{g m}^{-3}$ at the three PRD ground sites (PY, XK, and DG) and $7.68 \mu\text{g m}^{-3}$ at the elevated NC site, much higher than the average level ($2.88 \mu\text{g m}^{-3}$) observed at MFS, the mountaintop site. The same vertical spatial gradient was observed in the rainy season.

Table 2 compares BC mass concentrations as measured by Aethalometers in this study with those reported in the literature for other locations. The overall campaign average of BC at the four PRD urban/rural receptor sites is $9.48 \mu\text{g m}^{-3}$. As shown in Table 2, BC in the PRD is not the highest among urban areas in China, but the level is much higher than urban areas elsewhere in the world, such as Paris ($1.66 \mu\text{g m}^{-3}$) (Healy et al., 2012), New York ($1.38 \mu\text{g m}^{-3}$) (Venkatachari et al., 2006), and Mexico City ($3.4 \mu\text{g m}^{-3}$) (Salcedo et al., 2006).

The campaign average of BC at MFS is similar to the level reported for rural locations in China, such as Hong Kong ($2.4 \mu\text{g m}^{-3}$) (Cheng et al., 2006) and Beijing ($2.12 \mu\text{g m}^{-3}$) by Yan et al., 2008 and $2.37 \mu\text{g m}^{-3}$ by Zhou et al., 2009).

The BC level at YX Island is comparable to those reported for coastal areas in Europe, such as Baltic Sea ($0.6 \mu\text{g m}^{-3}$) (Bycenkiene et al., 2011) and Mediterranean ($\sim 0.7 \mu\text{g m}^{-3}$) (Saha and Despiau, 2009), but higher than those observed over southwest Indian Ocean ($0.43 \mu\text{g m}^{-3}$) (Bhugwant et al., 2000) and the Pacific Ocean ($0.006 \mu\text{g m}^{-3}$) (Bodhaine, 1995). The higher BC at YX may partially be attributed to emissions from passing-by marine vessels (Kaluza et al., 2010).

17385

3.3 Seasonal variation in BC

For the understanding of seasonal variation of BC, air mass back trajectories at the sampling locations were examined for all sampling days using the HYSPLIT-4 model (Draxler and Rolph, 2012). YX (16.33°N , 112.83°E), MFS (23.33°N , 113.48°E) and NC (23.00°N , 113.36°E) are selected as the reference points for the back trajectories calculation to represent the South China Sea and the PRD region. Height of 150 m is chosen to track the path of air masses which would eventually arrive at the NC and YX in the previous 72 h while for MFS the height was set as 535 m to represent the real situation. Figure 3 shows the back trajectories of air masses arriving at YX, MFS, and NC in both rainy and dry seasons.

During the rainy season PRD was significantly affected by two different air flows. For most of the time, PRD was affected by the southerly air flow that originated from the vast ocean. On a few days PRD was affected by the northeasterly air flow, which was related to specific weather systems such as typhoons and troughs. For example, during 15–22 May 2008, the tropical typhoon Halong (Fig. S3) was approaching the Philippines, and this large-scale weather system shifted the prevailing wind in PRD to northeasterly. During the dry season, PRD was influenced by the strong northeast monsoon, which brought polluted air masses from the more economically-developed regions in the eastern Asia. The seasonal difference in air mass origins is consistent with the large scale wind stream shown in Fig. 4. In rainy season the prevailing wind in South China and over the South China Sea is driven by the South China Sea monsoon while in dry season the wind direction is reversed. The reversed wind fields in the rainy and dry seasons result in different dispersion conditions in the PRD region.

As seen from the BC measurements, the monsoon system has a significant impact on the seasonal contrast in BC loading in the PRD urban region. Strong seasonal variations were seen at the ground sites (PY and DG) and the elevated site (NC) in PRD where measurements were available in both the rainy and dry seasons. The BC concentrations were significantly higher in the dry season, with an average of $12.65 \mu\text{g m}^{-3}$

17386

in the dry season and $5.83 \mu\text{g m}^{-3}$ in the rainy season. In comparison, the seasonal variations of BC at MFS were small. The average BC mass concentration at MFS was $2.62 \mu\text{g m}^{-3}$ in the rainy season vs. $2.88 \mu\text{g m}^{-3}$ in the dry season.

In the dry season MFS is upwind of the PRD region, making it an indicator for super-regional transport. Considering that air mass during cold front is cleaner as it comes from high altitude, the BC average excluding cold front days will be more appropriate to represent the influence from eastern China in dry season. This concentration ($3.19 \mu\text{g m}^{-3}$) is 20% higher than the rainy season ($2.62 \mu\text{g m}^{-3}$). This may imply that super-regional transport is not the major cause for elevated BC observed at the PRD urban areas in the dry season. The higher abundance of BC in the air may be associated with weaker dispersion conditions in winter (Wu et al., 2008), including wind speed reduction ($\sim 35\%$ lower than the rainy season in this study).

The seasonal variation of BC at YX Island was small, with an average BC of $0.54 \mu\text{g m}^{-3}$ in the rainy season and $0.67 \mu\text{g m}^{-3}$ in the dry season. In the rainy season, the north-central area of the South China Sea was mainly controlled by the South China Sea monsoon, which originated from the vast ocean. Occasionally in the rainy season, YX Island is under control of the northerly air flow related to the weather system activity, such as the period of 15–22 May (Fig. 3a). In the dry season YX is downwind of East China Sea, Taiwan Strait and part of the coastal areas of eastern China. The difference in air mass origins may explain the slightly higher BC level in the dry season than the rainy season.

3.4 BC Diurnal variation

Diurnal variations of BC are shown in Fig. 5 for the rainy and dry seasons. Two cold front events occurred during the sampling period, evidenced by elevated station pressure, rapid drop in temperature, and stronger wind (Fig. 2b). During the two cold front periods (period A: 22–24 December 2008; period B: 29 December 2008–3 January 2009), the

17387

diurnal pattern was very different from the overall diurnal pattern in dry season, so the cold front diurnal pattern is plotted separately in Fig. 5.

All the PRD sites showed a discernible bi-mode peak pattern, and the pattern was more prominent in the rainy season. At the continental urban/suburban sites, diurnal trends with one peak in the morning and the other in evening were observed. The lowest BC usually occurred in early afternoon in both rainy and dry seasons. This observation is consistent with observations reported in the previous studies conducted in PRD region (Andreae et al., 2008; Garland et al., 2008; Verma et al., 2010). Higher BC in night is a combined result of lower mixing height after sunset and increased emissions from diesel trucks in the evening, which are associated with the traffic regulation in this region (Garland et al., 2008). In the dry season, the evening peak at DG and XK was more pronounced and broader than the morning peak, with the evening peak extending to overlap the morning peak.

Passing cold fronts usually bring strong wind and clean air from high altitudes to the PRD region, resulting significant reductions in BC concentrations, which were observed across all the PRD sites as shown in Fig. 2b. During the cold front periods, the evening BC peak was larger than the morning peak at all PRD sites, which may be attributable to two causes. First, the activity intensity of heavy duty vehicles in nighttime was as high as daytime in Guangzhou urban areas till midnight (Verma et al., 2010). Second, the nighttime wind speed was weaker than daytime and the mixing height was lower in nighttime. These two factors acted together, making the nighttime peak more pronounced than the morning peak. As the strong wind during the cold front events would effectively carry away pollutants, providing an opportunity to reveal the fresh local emission pattern in one day. This pattern of peaking in the evening is consistent with the heavy duty vehicles activity pattern in urban Guangzhou (6:00–24:00 LT), as reported by Verma et al. (2010), implying the significance of BC emissions from the transportation sector. The identical diurnal pattern in DG and XK was consistent with their high inter-site correlation in the dry season ($r = 0.77$).

17388

At MFS, the PRD background site, the diurnal pattern in the dry season was very similar to those at the urban/suburban sites in PRD, but the diurnal pattern in the rainy season was hardly discernible.

A diurnal variation pattern in BC was discernible at YX, likely a result of operation pattern in the local diesel generator for power. The period with elevated BC coincided with the office hours (7:00–12:00 and 14:00–18:00 LT). During the non-office hours, BC was almost flat. The two peaks of BC were higher in the dry season.

3.5 BC Light absorption

Light absorption coefficients (σ_{abs}) data are summarized for the dry and rainy seasons separately in Table 3 and compared in Fig. S1. Daily average σ_{abs} across all sites varied from 4 to 352 Mm^{-1} during the sampling campaign. The continent average of σ_{abs} was tenfold that at the oceanic site YX island. σ_{abs} observations in this study are compared with those reported in previous studies in Table 3. σ_{abs} in Guangzhou during the dry season of 2009 was significantly higher than those measured in 2004 for both urban (188 Mm^{-1} in 2009 vs. 91 Mm^{-1} in 2004) and rural (119 Mm^{-1} in 2009 vs. 70 Mm^{-1} in 2004) sites (Andreae et al., 2008; Cheng et al., 2008). The observed σ_{abs} at MFS, a background site in PRD, was 26 Mm^{-1} in the rainy season and 29 Mm^{-1} in the dry season, lower than previous observations in the northern rural area of city Guangzhou (42.5 Mm^{-1}) (Garland et al., 2008), comparable to those found in Yangtze Delta (23 Mm^{-1}) (Xu et al., 2002) and in North China Plain (17.5 Mm^{-1}) (Yan et al., 2008), but higher than those in South East Asia (15 Mm^{-1}) (Li et al., 2012). The σ_{abs} observed at the PRD urban area is much higher than those in urban areas around the world, e.g., Mexico City (Marley et al., 2009), Tokyo (Nakayama et al., 2010) and a few US cities (Chow et al., 2009; Thompson et al., 2012).

17389

4 Summary

We report in this work the observations of BC concentrations and absorption coefficients (σ_{abs}) by aethalometers in Yongxing Island of the South China Sea (a superregional background site) and five continental locations in southern China mainland in the rainy season and dry season of 2008. BC loading at the South China Sea background site showed little seasonal difference between the dry and rainy seasons, with an average of $0.54 \mu\text{g m}^{-3}$ in the rainy season and $0.67 \mu\text{g m}^{-3}$ in the dry season. Light absorption at YX is comparable but a bit higher than other coastal areas around the world. The BC level at the PRD background site (Maofengshan at 535 m a.s.l.) also had a small seasonal difference, with $2.88 \mu\text{g m}^{-3}$ in the dry season and $2.66 \mu\text{g m}^{-3}$ in the rainy season. The level at this regional background site is very similar to those found in North China Plain. The seasonal average concentration of BC in the PRD urban area is $12.65 \mu\text{g m}^{-3}$ in the dry season and a significantly lower level ($5.72 \mu\text{g m}^{-3}$) was found in the rainy season. The BC level in the PRD region is much higher than other urban areas around the world. Inter-site correlation analysis of BC measurements revealed that BC was a regional pollutant. The seasonal dependency of inter-site correlations implies that the monsoon systems play an important role in transport and spatial distribution of BC. A bi-peak diurnal pattern was observed at all the PRD sites, and the pattern is more prominent in the urban areas. The first peak usually appears during the early morning rush hours and the second peak shows up in the evening. Our analysis suggests that the diurnal variation pattern is mainly a result of vehicular emissions.

Supplementary material related to this article is available online at:
<http://www.atmos-chem-phys-discuss.net/13/17375/2013/acpd-13-17375-2013-supplement.pdf>

Acknowledgements. This study is supported by Project 973 (2011CB403403) and Natural Science Foundation of China (40775011, U0733004). The authors gratefully acknowledge the

17390

References

- Andreae, M. O.: The dark side of aerosols, *Nature*, 409, 671–672, 2001.
- 5 Andreae, M. O., Schmid, O., Yang, H., Chand, D., Yu, J. Z., Zeng, L. M., and Zhang, Y. H.: Optical properties and chemical composition of the atmospheric aerosol in urban Guangzhou, China, *Atmos. Environ.*, 42, 6335–6350, 2008.
- Babu, S. S. and Moorthy, K. K.: Anthropogenic impact on aerosol black carbon mass concentration at a tropical coastal station: a case study, *Curr. Sci. India*, 81, 1208–1214, 2001.
- 10 Bhugwant, C., Cachier, H., Bessafi, M., and Laveau, J.: Impact of traffic on black carbon aerosol concentration at la Reunion Island (Southern Indian Ocean), *Atmos. Environ.*, 34, 3463–3473, 2000.
- Bodhaine, B. A.: Aerosol absorption-measurements at Barrow, Mauna-Loa and the South-Pole, *J. Geophys. Res.-Atmos.*, 100, 8967–8975, 1995.
- 15 Bycenkiene, S., Ulevicius, V., and Kecorius, S.: Characteristics of black carbon aerosol mass concentration over the East Baltic region from two-year measurements, *J. Environ. Monitor.*, 13, 1027–1038, doi:10.1039/C0em00480d, 2011.
- Cao, J. J., Lee, S. C., Ho, K. F., Zou, S. C., Fung, K., Li, Y., Watson, J. G., and Chow, J. C.: Spatial and seasonal variations of atmospheric organic carbon and elemental carbon in Pearl River Delta Region, China, *Atmos. Environ.*, 38, 4447–4456, doi:10.1016/j.atmosenv.2004.05.016, 2004.
- 20 Cao, J. J., Zhu, C. S., Chow, J. C., Watson, J. G., Han, Y. M., Wang, G. H., Shen, Z. X., and An, Z. S.: Black carbon relationships with emissions and meteorology in Xi'an, China, *Atmos. Res.*, 94, 194–202, doi:10.1016/j.atmosres.2009.05.009, 2009.
- 25 Cheng, Y., Lee, S. C., Ho, K. F., Wang, Y. Q., Cao, J. J., Chow, J. C., and Watson, J. G.: Black carbon measurement in a coastal area of south China, *J. Geophys. Res.-Atmos.*, 111, D12310, doi:10.1029/2005jd006663, 2006.
- Cheng, Y. F., Wiedensohler, A., Eichler, H., Su, H., Gnauk, T., Brueggemann, E., Herrmann, H., Heintzenberg, J., Slanina, J., Tuch, T., Hu, M., and Zhang, Y. H.: Aerosol optical properties

17391

- and related chemical apportionment at Xinken in Pearl River Delta of China, *Atmos. Environ.*, 42, 6351–6372, doi:10.1016/j.atmosenv.2008.02.034, 2008.
- Chi, X. G., Duan, F. K., Dong, S. P., Liu, X. D., and Yu, T.: Concentration level and seasonal variation of organic carbon and elemental carbon in Beijing aerosols, *Environmental Monitoring in China*, 16, 35–38, 2000 (in Chinese).
- 5 Chow, J. C., Watson, J. G., Doraiswamy, P., Chen, L. W. A., Sodeman, D. A., Lowenthal, D. H., Park, K., Arnott, W. P., and Motallebi, N.: Aerosol light absorption, black carbon, and elemental carbon at the Fresno Supersite, California, *Atmos. Res.*, 93, 874–887, doi:10.1016/j.atmosres.2009.04.010, 2009.
- 10 Chung, C. E., Kim, S.-W., Lee, M., Yoon, S.-C., and Lee, S.: Carbonaceous aerosol AAE inferred from in-situ aerosol measurements at the Gosan ABC super site, and the implications for brown carbon aerosol, *Atmos. Chem. Phys.*, 12, 6173–6184, doi:10.5194/acp-12-6173-2012, 2012.
- Collaud Coen, M., Weingartner, E., Apituley, A., Ceburnis, D., Fierz-Schmidhauser, R., Flen-tje, H., Henzing, J. S., Jennings, S. G., Moerman, M., Petzold, A., Schmid, O., and Baltensperger, U.: Minimizing light absorption measurement artifacts of the Aethalometer: evaluation of five correction algorithms, *Atmos. Meas. Tech.*, 3, 457–474, doi:10.5194/amt-3-457-2010, 2010.
- Draxler, R. R. and Rolph, G. D.: HYSPLIT (HYbrid Single-Particle Lagrangian Integrated Trajectory) Model access via NOAA ARL READY Website, available at: <http://ready.arl.noaa.gov/HYSPLIT.php>, NOAA Air Resources Laboratory, Silver Spring, MD, 2012.
- Engling, G. and Gelencser, A.: Atmospheric brown clouds: from local air pollution to climate change, *Elements*, 6, 223–228, doi:10.2113/gselements.6.4.223, 2010.
- Garland, R. M., Yang, H., Schmid, O., Rose, D., Nowak, A., Achtert, P., Wiedensohler, A., Takegawa, N., Kita, K., Miyazaki, Y., Kondo, Y., Hu, M., Shao, M., Zeng, L. M., Zhang, Y. H., Andreae, M. O., and Pöschl, U.: Aerosol optical properties in a rural environment near the mega-city Guangzhou, China: implications for regional air pollution, radiative forcing and remote sensing, *Atmos. Chem. Phys.*, 8, 5161–5186, doi:10.5194/acp-8-5161-2008, 2008.
- 25 Gundel, L. A., Dod, R. L., Rosen, H., and Novakov, T.: The relationship between optical attenuation and black carbon concentration for ambient and source particles, *Sci. Total Environ.*, 36, 197–202, 1984.
- 30 Healy, R. M., Sciare, J., Poulain, L., Kamili, K., Merkel, M., Müller, T., Wiedensohler, A., Eckhardt, S., Stohl, A., Sarda-Estève, R., McGillicuddy, E., O'Connor, I. P., Sodeau, J. R., and

17392

- Wenger, J. C.: Sources and mixing state of size-resolved elemental carbon particles in a European megacity: Paris, *Atmos. Chem. Phys.*, 12, 1681–1700, doi:10.5194/acp-12-1681-2012, 2012.
- IPCC: *Climate Change 1995: the Science of Climate Change*, Cambridge University Press, Cambridge, New York, xii, 572 pp., 1996.
- Jacobson, M. Z.: Strong radiative heating due to the mixing state of black carbon in atmospheric aerosols, *Nature*, 409, 695–697, 2001.
- Kaluza, P., Kolzsch, A., Gastner, M. T., and Blasius, B.: The complex network of global cargo ship movements, *J. R. Soc. Interface*, 7, 1093–1103, doi:10.1098/rsif.2009.0495, 2010.
- Kirchstetter, T. W., Novakov, T., and Hobbs, P. V.: Evidence that the spectral dependence of light absorption by aerosols is affected by organic carbon, *J. Geophys. Res.-Atmos.*, 109, D21208, doi:10.1029/2004jd004999, 2004.
- Kozlov, V., Panchenko, M., and Yausheva, E.: Diurnal variations of the submicron aerosol and black carbon in the near-ground layer, *Atmospheric and Oceanic Optics*, 24, 30–38, doi:10.1134/s102485601101009x, 2011.
- Lack, D. A. and Cappa, C. D.: Impact of brown and clear carbon on light absorption enhancement, single scatter albedo and absorption wavelength dependence of black carbon, *Atmos. Chem. Phys.*, 10, 4207–4220, doi:10.5194/acp-10-4207-2010, 2010.
- Li, C., Tsay, S.-C., Hsu, N. C., Kim, J. Y., Howell, S. G., Huebert, B. J., Ji, Q., Jeong, M.-J., Wang, S.-H., Hansell, R. A., and Bell, S. W.: Characteristics and composition of atmospheric aerosols in Phimai, central Thailand during BASE-ASIA, *Atmos. Environ.*, doi:10.1016/j.atmosenv.2012.04.003, in press, 2012.
- Lohmann, U. and Lesins, G.: Stronger constraints on the anthropogenic indirect aerosol effect, *Science*, 298, 1012–1015, 2002.
- Lou, S. J., Mao, J. T., and Wang, M. H.: Observational study of black carbon aerosol in Beijing, *Acta Scientiae Circumstantiae*, 25, 17–22, 2005.
- Müller, T., Henzing, J. S., de Leeuw, G., Wiedensohler, A., Alastuey, A., Angelov, H., Bizjak, M., Collaud Coen, M., Engström, J. E., Gruening, C., Hillamo, R., Hoffer, A., Imre, K., Ivanow, P., Jennings, G., Sun, J. Y., Kalivitis, N., Karlsson, H., Komppula, M., Laj, P., Li, S.-M., Lunder, C., Marinoni, A., Martins dos Santos, S., Moerman, M., Nowak, A., Ogren, J. A., Petzold, A., Pichon, J. M., Rodriguez, S., Sharma, S., Sheridan, P. J., Teinilä, K., Tuch, T., Viana, M., Virkkula, A., Weingartner, E., Wilhelm, R., and Wang, Y. Q.: Characterization and intercom-

17393

- parison of aerosol absorption photometers: result of two intercomparison workshops, *Atmos. Meas. Tech.*, 4, 245–268, doi:10.5194/amt-4-245-2011, 2011.
- Ma, N., Zhao, C. S., Nowak, A., Müller, T., Pfeifer, S., Cheng, Y. F., Deng, Z. Z., Liu, P. F., Xu, W. Y., Ran, L., Yan, P., Göbel, T., Hallbauer, E., Mildenerger, K., Henning, S., Yu, J., Chen, L. L., Zhou, X. J., Stratmann, F., and Wiedensohler, A.: Aerosol optical properties in the North China Plain during HaChi campaign: an in-situ optical closure study, *Atmos. Chem. Phys.*, 11, 5959–5973, doi:10.5194/acp-11-5959-2011, 2011.
- Man, C. K. and Shih, M. Y.: Light scattering and absorption properties of aerosol particles in Hong Kong, *J. Aerosol. Sci.*, 32, 795–804, 2001.
- Marley, N. A., Gaffney, J. S., Castro, T., Salcido, A., and Frederick, J.: Measurements of aerosol absorption and scattering in the Mexico City Metropolitan Area during the MILAGRO field campaign: a comparison of results from the T0 and T1 sites, *Atmos. Chem. Phys.*, 9, 189–206, doi:10.5194/acp-9-189-2009, 2009.
- Menon, S., Hansen, J., Nazarenko, L., and Luo, Y. F.: Climate effects of black carbon aerosols in China and India, *Science*, 297, 2250–2253, 2002.
- Moosmüller, H., Chakrabarty, R. K., and Arnott, W. P.: Aerosol light absorption and its measurement: a review, *J. Quant. Spectrosc. Ra.*, 110, 844–878, 2009.
- Moosmüller, H., Chakrabarty, R. K., Ehlers, K. M., and Arnott, W. P.: Absorption Ångström coefficient, brown carbon, and aerosols: basic concepts, bulk matter, and spherical particles, *Atmos. Chem. Phys.*, 11, 1217–1225, doi:10.5194/acp-11-1217-2011, 2011.
- Nakayama, T., Hagino, R., Matsumi, Y., Sakamoto, Y., Kawasaki, M., Yamazaki, A., Uchiyama, A., Kudo, R., Moteki, N., Kondo, Y., and Tonokura, K.: Measurements of aerosol optical properties in central Tokyo during summertime using cavity ring-down spectroscopy: comparison with conventional techniques, *Atmos. Environ.*, 44, 3034–3042, doi:10.1016/j.atmosenv.2010.05.008, 2010.
- Niu, S. J. and Zhang, Q. Y.: Scattering and absorption coefficients of aerosols in a semi-arid area in China: diurnal cycle, seasonal variability and dust events, *Asia-Pac. J. Atmos. Sci.*, 46, 65–71, doi:10.1007/s13143-010-0007-2, 2010.
- Pandolfi, M., Cusack, M., Alastuey, A., and Querol, X.: Variability of aerosol optical properties in the Western Mediterranean Basin, *Atmos. Chem. Phys.*, 11, 8189–8203, doi:10.5194/acp-11-8189-2011, 2011.
- Penner, J. E., Dong, X. Q., and Chen, Y.: Observational evidence of a change in radiative forcing due to the indirect aerosol effect, *Nature*, 427, 231–234, doi:10.1038/Nature02234, 2004.

17394

- Qin, S. G., Tang, J., and Wen, Y. P.: Black carbon and its importance in climate change studies, *Meteorology*, 27, 3–7, 2001 (in Chinese).
- Ramanathan, V. and Carmichael, G.: Global and regional climate changes due to black carbon, *Nat. Geosci.*, 1, 221–227, doi:10.1038/Ngeo156, 2008.
- 5 Ramanathan, V., Crutzen, P. J., Mitra, A. P., and Sikka, D.: The Indian Ocean Experiment and the Asian brown cloud, *Curr. Sci. India*, 83, 947–955, 2002.
- Reddy, M. S. and Venkataraman, C.: Atmospheric optical and radiative effects of anthropogenic aerosol constituents from India, *Atmos. Environ.*, 34, 4511–4523, 2000.
- Saha, A. and Despiou, S.: Seasonal and diurnal variations of black carbon aerosols over
10 a Mediterranean coastal zone, *Atmos. Res.*, 92, 27–41, doi:10.1016/j.atmosres.2008.07.007, 2009.
- Salcedo, D., Onasch, T. B., Dzepina, K., Canagaratna, M. R., Zhang, Q., Huffman, J. A., De-
Carlo, P. F., Jayne, J. T., Mortimer, P., Worsnop, D. R., Kolb, C. E., Johnson, K. S., Zu-
berl, B., Marr, L. C., Volkamer, R., Molina, L. T., Molina, M. J., Cardenas, B., Bernabé, R. M.,
15 Márquez, C., Gaffney, J. S., Marley, N. A., Laskin, A., Shutthanandan, V., Xie, Y., Brune, W.,
Leshner, R., Shirley, T., and Jimenez, J. L.: Characterization of ambient aerosols in Mexico
City during the MCMA-2003 campaign with Aerosol Mass Spectrometry: results from the
CENICA Supersite, *Atmos. Chem. Phys.*, 6, 925–946, doi:10.5194/acp-6-925-2006, 2006.
- Sun, H., Zhang, Z., Pei, L. M., and Miao, W. Q.: A preliminary investigation of the pollution of
20 organic carbon and elemental carbon in aerosol in Qiqihar, *Journal of Science of Teachers
College and University*, 17, 57–61, 1997 (in Chinese).
- Tang, J., Wen, Y. P., Zhou, L. X., Qi, D. L., Zheng, M., Trivett, N., and Wallgren, E.: Observational
study of black carbon in clean air area of western China, *Journal of Applied Meteorological
Science*, 10, 160–170, 1999 (in Chinese).
- 25 Thompson, J. E., Hayes, P. L., Jimenez, K. A. J. L., Zhang, X., Liu, J., Weber, R. J., and
Buseck, P. R.: Aerosol optical properties at Pasadena, CA during CalNex 2010, *Atmos. Enviro-
n.*, 55, 190–200, doi:10.1016/j.atmosenv.2012.03.011, 2012.
- Venkatachari, P., Zhou, L. M., Hopke, P. K., Felton, D., Rattigan, O. V., Schwab, J. J., and De-
merjian, K. L.: Spatial and temporal variability of black carbon in New York City, *J. Geophys.
30 Res.-Atmos.*, 111, D10S05, doi:10.1029/2005jd006314, 2006.
- Verma, R. L., Sahu, L. K., Kondo, Y., Takegawa, N., Han, S., Jung, J. S., Kim, Y. J., Fan, S., Sugi-
moto, N., Shammaa, M. H., Zhang, Y. H., and Zhao, Y.: Temporal variations of black carbon in

17395

- Guangzhou, China, in summer 2006, *Atmos. Chem. Phys.*, 10, 6471–6485, doi:10.5194/acp-
10-6471-2010, 2010.
- Wang, G. C., Kong, Q. X., Ren, L. X., Gu, Z. F., and Emilenko, A.: Black carbon aerosol and
its variations in the urban atmosphere in Beijing area, *The Chinese Journal of Process En-
5 gineering*, 2, 284–288, 2002.
- Watson, J. G. and Chow, J. C.: Comparison and evaluation of in situ and filter car-
bon measurements at the Fresno Supersite, *J. Geophys. Res.-Atmos.*, 107, 8341,
doi:10.1029/2001jd000573, 2002.
- Wu, D.: A discussion on difference between haze and fog and warning of ash haze weather,
10 *Meteorological Monthly*, 31, 3–7, 2005 (in Chinese).
- Wu, D., Tie, X. X., Li, C. C., Ying, Z. M., Lau, A. K. H., Huang, J., Deng, X. J., and Bi, X. Y.: An
extremely low visibility event over the Guangzhou region: a case study, *Atmos. Environ.*, 39,
6568–6577, doi:10.1016/j.atmosenv.2005.07.061, 2005.
- Wu, D., Bi, X. Y., Deng, X. J., Li, F., Tan, H. B., Liao, G. L., and Huang, J.: Effect of atmospheric
15 haze on the deterioration of visibility over the Pearl River Delta, *Acta Meteorol. Sin.*, 21, 215–
223, 2007.
- Wu, D., Liao, G., Deng, X., Bi, X., Tan, H., Li, F., Jiang, C., Xia, D., and Fan, S.: Transport
condition of surface layer under haze weather over the Pearl River Delta, *Journal of Applied
Meteorological Science*, 19, 1–9, 2008 (in Chinese).
- 20 Wu, D., Mao, J. T., Deng, X. J., Tie, X. X., Zhang, Y. H., Zeng, L. M., Li, F., Tan, H. B., Bi, X. Y.,
Huang, X. Y., Chen, J., and Deng, T.: Black carbon aerosols and their radiative properties
in the Pearl River Delta region, *Sci. China Ser. D*, 52, 1152–1163, doi:10.1007/s11430-009-
0115-y, 2009.
- Xu, J., Bergin, M. H., Yu, X., Liu, G., Zhao, J., Carrico, C. M., and Baumann, K.: Measurement
25 of aerosol chemical, physical and radiative properties in the Yangtze delta region of China,
Atmos. Environ., 36, 161–173, 2002.
- Yan, P., Tang, J., Huang, J., Mao, J. T., Zhou, X. J., Liu, Q., Wang, Z. F., and Zhou, H. G.: The
measurement of aerosol optical properties at a rural site in Northern China, *Atmos. Chem.
Phys.*, 8, 2229–2242, doi:10.5194/acp-8-2229-2008, 2008.
- 30 Zhou, X. H., Cao, J., Wang, T., Wu, W. S., and Wang, W. X.: Measurement of black carbon
aerosols near two Chinese megacities and the implications for improving emission invento-
ries, *Atmos. Environ.*, 43, 3918–3924, doi:10.1016/j.atmosenv.2009.04.062, 2009.

17396

17397

Table 1. Inter-site correlation (Pearson's r) of hourly light absorption data in the Pearl River Delta Region.

Pair	Rainy Season	Dry Season
NC vs. PY	0.83	0.49
NC vs. MFS	-0.17	0.30
NC vs. DG	0.66	0.72
NC vs. XK		0.70
MFS vs. PY	-0.21	0.48
MFS vs. XK		0.09
MFS vs. DG	-0.11	0.17
PY vs. XK		0.41
PY vs. DG	0.65	0.48
XK vs. DG		0.77

17398

Table 2. Comparison of BC concentrations ($\mu\text{g m}^{-3}$) obtained by aethalometers at different locations in the world.

Location	Site Characteristics	Sampling Period	Inlet	BC mass	Correction ¹	Reference
Yongxing Island (YX), China	Oceanic rural, (South China Sea)	May–Jun 2008	PM _{2.5}	0.54	Yes	This work
Maofengshan (MFS), Guangzhou, China	Rural, (Pearl River Delta)	Dec 2008–Jan 2009	PM ₁₀	0.67	Yes	This work
		May–Jun 2008	PM ₁₀	2.62		
Nancun (NC), Guangzhou, China	Suburban, (Pearl River Delta)	Dec 2008–Jan 2009	PM ₁₀	2.88	Yes	This work
		May–Jun 2008		5.57		
Panyu (PY), Guangzhou, China	Urban, (Pearl River Delta)	Dec 2008–Jan 2009	PM ₁₀	7.68	Yes	Wu et al. (2009)
		May–Jun 2008		8.86		
Dongguan (DG), China	Suburban, (Pearl River Delta)	Dec 2008–Jan 2009	PM ₁₀	20.21	Yes	This work
		May–Jun 2008		4.86		
Xinken (XK), Guangzhou, China	Rural, (Pearl River Delta)	Dec 2008–Jan 2009	PM ₁₀	10.11	Yes	This work
		Dec 2008–Jan 2009		12.61		
Yangshuo (YS), China	Urban (Guangxi)	May–Jun 2008	PM _{2.5}	6.93	Yes	This work
Hong Kong, China	Coastal Rural (Pearl River Delta)	Jun 2004–May 2005	PM _{2.5}	2.4	No	Cheng et al. (2006)
Mauna Loa, USA	Oceanic rural (Pacific Ocean)	1990–1993	/	0.006	Yes	Bodhaine (1995)
Toulon, France	Urban Coastal (Mediterranean)	2005 Winter	PM _{2.5}	0.95	No	Saha and Despiou (2009)
		2006 Summer	/	0.45		
La Réunion Island, French	Urban Coastal (Indian Ocean)	Nov 1996 Apr, Sep 1998	/	0.43	No	Bhugwant et al. (2000)
Preila, Lithuania	Coastal Rural (Baltic Sea)	2008–2009	PM _{2.5}	0.6	No	Bycenkiene et al. (2011)
Xilinhot, China	Rural (XilinGol League grassland)	Apr 2005	/	2	No	Niu and Zhang (2010)
Shangdianzi, China	Rural (Beijing, North China Plain)	Dec 2005	TSP	6.2	Yes	Yan et al. (2008)
		Apr 2003–Jan 2005		2.12		
Changping, China	Rural (Beijing, North China Plain)	Jun–Jul 2005	PM _{2.5}	2.37	No	Zhou et al. (2009)
Taicang, China	Suburban (Shanghai Yangtze delta)	May–Jun 2005	/	5.47		
Xi'an, China	Suburban (Guanzhong Plain)	Sep 2003–Aug 2005	PM _{2.5}	14.7	No	Cao et al. (2009)
Fresno, USA	Urban	Jan–Dec 2000	PM _{2.5}	1.17	No	Watson and Chow (2002)
New York, USA	Urban	Jan–Feb 2004	/	1.38	No	Venkatachari et al. (2006)
Paris, France	Urban	Jan–Feb 2010	PM _{2.5}	1.66	Yes	Healy et al. (2012)
Mexico City, Mexico	Urban	Apr 2003	PM _{2.5}	3.4	No	Salcedo et al. (2006)
Tomsrsk, Russia	Urban	Summer 1997–2008	PM ₁	1.9	No	Kozlov et al. (2011)
		Winter 1997–2008	/	0.8		

¹ Correction refers to amendment of aethalometer measurements due to sampling artifacts related to aerosol loading, filter matrix and scattering effect (Coen et al., 2010).

17399

Table 3. Comparison of light absorption measurements (Mm^{-1}) at different locations in the world.

Location	Site characteristics	Sampling Duration	Inlet	Method ¹	$\sigma_{\text{abs}} \pm \text{std}$ @ wavelength	Correction ⁷	Reference
Yongxing Island (YX), China	Oceanic rural, (South China Sea)	May–Jun 2008	PM _{2.5}	AE	7.21 ± 5.23 @ 532 nm ²	Yes	This work
Maofengshan (MFS), Guangzhou, China	Rural, (Pearl River Delta)	Dec 2008–Jan 2009	PM ₁₀	AE	8.37 ± 5.88 @ 532 nm ²	Yes	This work
		May–Jun 2008	PM ₁₀	AE	26.45 ± 13.88 @ 532 nm ²		
Nancun (NC), Guangzhou, China	Suburban, (Pearl River Delta)	Dec 2008–Jan 2009	PM ₁₀	AE	28.77 ± 12.71 @ 532 nm ²	Yes	This work
		May–Jun 2008			53.47 ± 34.27 @ 532 nm ²		
Panyu (PY), Guangzhou, China	Urban (Pearl River Delta)	Dec 2008–Jan 2009	PM ₁₀	AE	73.10 ± 44.64 @ 532 nm ²	Yes	This work
		May–Jun 2008			84.03 ± 53.20 @ 532 nm ²		
Dongguan (DG), China	Suburban, (Pearl River Delta)	Dec 2008–Jan 2009	PM ₁₀	AE	188.80 ± 117.30 @ 532 nm ²	Yes	This work
		May–Jun 2008			47.10 ± 34.44 @ 532 nm ²		
Xinken (XK), Guangzhou, China	Rural, (Pearl River Delta)	Dec 2008–Jan 2009	PM ₁₀	AE	95.53 ± 60.88 @ 532 nm ²	Yes	This work
Yangshuo (YS), China	Urban (Guangxi)	May–Jun 2008	PM _{2.5}	AE	118.63 ± 73.90 @ 532 nm ²	Yes	This work
Nancun (NC), Guangzhou, China	Suburban	2004–2007 (Rainy season)	PM ₁₀	AE	66.20 ± 32.18 @ 532 nm ²	Yes	Wu et al. (2009)
		2004–2007 (Dry season)	PM ₁₀	AE	77 ± 21 @ 532 nm ²		
Guangzhou, China	Urban (Pearl River Delta)	5 Oct–5 Nov 2004	PM _{2.5}	PAS	88 ± 24 @ 532 nm ²	/	Andreea et al. (2008)
Xinken, Guangzhou, China	Rural (Pearl River Delta)	4 Oct–5 Nov 2004	PM ₁₀	MAAP	91 ± 60 @ 532 nm	/	Cheng et al. (2008)
Backgarden, Guangzhou, China	Rural (Pearl River Delta)	Jul 2006	PM ₁₀	PAS	70 ± 42 @ 550 nm ³	/	Garland et al. (2008)
Hong Kong, China	Coastal rural (Pearl River Delta)	May–Jun 1998	TSP	PSAP	42.5 ± 56.5 @ 532 nm	No	Man and Shih (2001)
Mauna Loa, USA	Oceanic rural (Pacific Ocean)	1990–1993	/	AE	7.65 @ 565 nm		
Barrow, USA	Coastal rural (Arctic Region)	1988–1993	/	AE	31.57 @ 565 nm	Yes	Bodhaine (1995)
Shangdianzi, Beijing, China	Rural (North China Plain)	Apr 2003–Jan 2005	TSP	AE	0.058 @ 550 nm		
Wuqing, Tianjing, China	Suburban (North China Plain)	Mar–Apr 2011	PM ₁₀	MAAP	17.5 ± 13.4 @ 525 nm	Yes	Yan et al. (2008)
Lin'an, Hangzhou, China	Rural (Yangtze delta)	Jul–Aug 2011	PM _{2.5}	PSAP	47 ± 38 @ 637 nm ⁴	Yes	Xu et al. (2002)
		Nov 1999			43 ± 27 @ 637 nm ⁴		
Phimai, Thailand	Rural (Indochinese peninsula)	Feb–May 2006	PM _{2.5}	AE	23 ± 14 @ 550 nm	Yes	Li et al. (2012)
Montseny, Spin Tokyo, Japan	Rural (Mediterranean)	Nov 2009–Oct 2010	PM ₁₀	MAAP	15 ± 8 @ 550 nm	Yes	Pandolfi et al. (2011)
		Aug 2007	PM ₁₀	PSAP	2.8 ± 2.2 @ 637 nm		
Mexico City, Mexico	Urban	Mar 2006	/	MAAP	13.6 ± 9.2 @ 532 nm ⁵	/	Nakayama et al. (2010)
Fresno, CA, USA	Urban	Aug–Sep 2005	PM _{2.5}	PA	37 @ 550 nm ⁶	/	Marley et al. (2009)
Pasadena, CA, USA	Urban	May–Jun 2010	PM _{2.5}	AM	5.22 @ 532 nm	Yes	Chow et al. (2009)
					4 @ 532 nm	/	Thompson et al. (2012)

¹ AE: Aethalometer; PAS: Photo Acoustic Spectrometer; MAAP: Multi Angle Absorption Photometer; PSAP: Particle Soot Absorption Photometer; AM: Albedo Meter.

² σ_{abs} reported at 532 nm is calculated from 880 nm measurement following an empirical formula reported by Wu et al. (2009).

³ σ_{abs} reported at 550 nm by Cheng et al. (2008) was calculated from MAAP measurement at 630 nm following power law (assuming AAE of soot as 1).

⁴ During the GAW2005 workshop, it was reported that the operation wavelength of MAAP was 637 nm rather than 670 nm as stated by the manufacturer (Müller et al., 2011).

⁵ σ_{abs} reported at 532 nm by was calculated from PSAP measurement at 565 nm following power law (assuming AAE of soot as 1).

⁶ The MAAP result was converted to 550 nm by the power law. The absorption Angstrom coefficients were obtained from 71 Aethalometer (Marley et al., 2009).

⁷ Correction refers to amendment of measurements due to sampling artifacts related to aerosol loading, filter matrix and scattering effect for the filter based instrument (e.g. AE, PSAP) (Coen et al., 2010).

17400

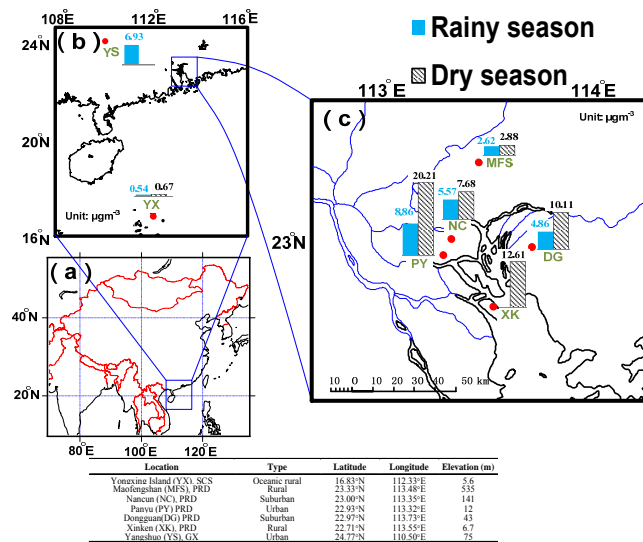


Fig. 1. Average black carbon concentrations during rainy and dry seasons across different sampling sites in column plots on the map (column plots in different maps are on the same scale and the unit of the associated numbers is $\mu\text{g m}^{-3}$). In a subtropical region like the Pearl River Delta (PRD), dry season is from October to April of the following year. Rainy season is from May to September. The enclosed table summarizes characteristics of the sampling sites in this study. **(a)** Location of the study region in China. **(b)** Location of the two short-term sites: the oceanic site at Yongxing Island (YX) and the urban site Yangshuo (YS). **(c)** Location of the long-term sites in PRD, including Maofengshan (MFS), Nancun (NC), Panyu, (PY), Dongguan (DG), Xinken (XK).

17401

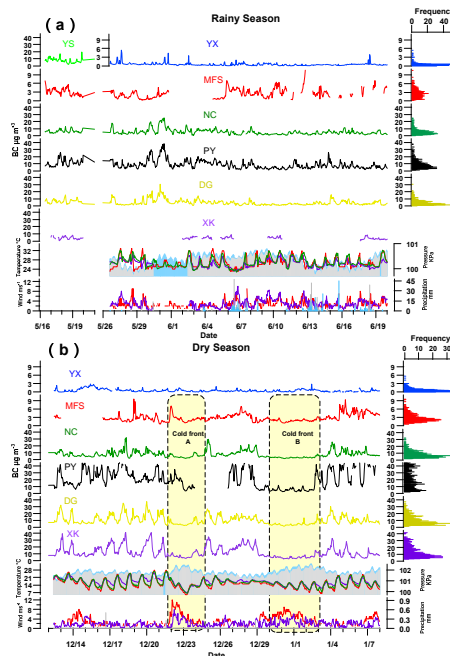


Fig. 2. Time series of BC hourly concentrations, temperature, atmospheric pressure, and wind speed in **(a)** rainy season **(b)** dry season. The histograms shown to the right of BC time series are the frequency distributions of BC concentrations. In the temperature time series plots, the red curve is measurements for Baiyun airport, 17 km west to MFS, and is considered to represent meteorological conditions in the northern part of PRD; the green curve is for NC and the purple curve is for XK. In the station pressure plots, the grey areas represent XK and the light blue for NC. In the wind speed plots, red is for Baiyun airport, purple for XK and precipitation (grey bars for XK, light blue for urban Guangzhou).

17402

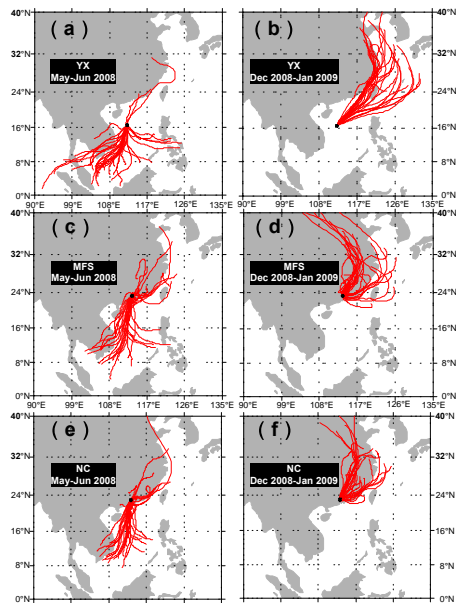


Fig. 3. The back trajectories (72 h) of air masses arriving at Yongxing Island and the Pearl River Delta. **(a)** Yongxing (YX) island (150 m.a.s.l.) from 16 May 2008 to 20 June 2008; **(b)** Yongxing (YX) Island (150 m.a.s.l.) from 12 December 2008 to 8 January 2009; **(c)** Maofengshan (MFS) (535 m.a.s.l.) from 16 May 2008 to 20 June 2008; **(d)** Maofengshan (MFS) (535 m.a.s.l.) from 12 December 2008 to 8 January 2009; **(e)** Nancun (NC) (150 m.a.s.l.) from 16 May 2008 to 20 June 2008; **(f)** Nancun (NC) (150 m.a.s.l.) from 12 December 2008 to 8 January 2009.

17403

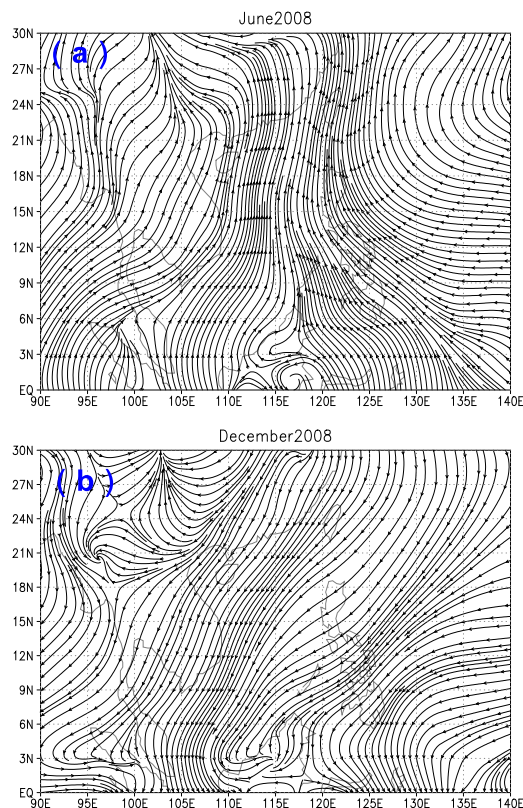


Fig. 4. South China Sea monthly average wind stream maps in **(a)** June 2008, South China Sea monsoon and **(b)** December 2008, Northeast monsoon.

17404

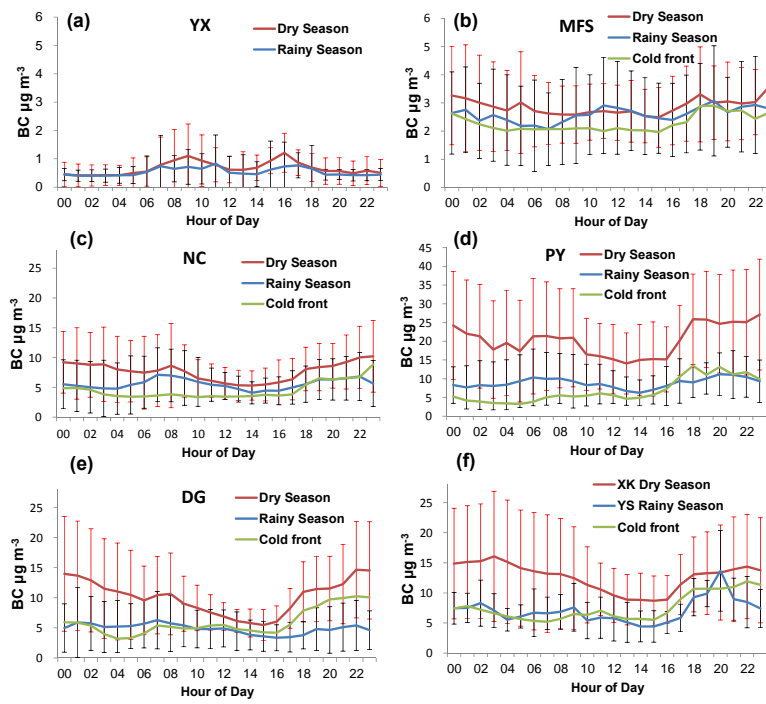


Fig. 5. Diurnal variations of BC concentrations at six monitoring sites in rainy season, dry seasons and during cold front. The sites are (a) Yongxing island (YX), (b) Maofengshan (MFS), (c) Nancun (NC), (d) Panyu (PY), (e) Dongguan (DG), and (f) Xinken (XK) in dry season and Yangshuo (YS) in rainy season